JOURNAL OF SOLID STATE CHEMISTRY **51**, 300–306 (1984)

ESR Evidence for Structural Rearrangements Occurring upon MoO_3 Reduction

EWA SERWICKA

Institute of Catalysis and Surface Chemistry, Polish Academy of Sciences, 30-239 Krakow, ul.Niezapominajek, Poland

Received January 4, 1983, and in revised form August 29, 1983

Reduction of polycrystalline MoO_3 in the course of heat treatment *in vacuo* has been studied by means of ESR. The formation of two different Mo(V) centers has been identified: center A with $g_x = 1.946$, $g_y = 1.960$, $g_z = 1.868$; and center B characterized by $g_x = 1.943$, $g_y = 1.954$, $g_z = 1.878$. Center B exhibited a well-resolved hyperfine structure resulting from naturally abundant odd isotopes of Mo: $A_x = 3.2$ mT, $A_y = 3.0$ mT, $A_z = 7.0$ mT. Species A formed at an early stage of reduction has been identified as Mo(V) in rhombically distorted square pyramidal surrounding, whereas center B appearing in strongly reduced samples shows a distorted octahedral coordination. The results have been interpreted in terms of the crystallographic shear mechanism.

Introduction

The mechanism of MoO_3 reduction has been, for a long time, a subject of widespread interest because of particularly high oxygen mobility observed for this oxide (*1–6*). This phenomenon has been found to be closely connected with catalytic properties of molybdena based catalysts (*4, 7–11*). It has been suggested that the facility with which oxygen can be released and absorbed by MoO_3 may be associated with the formation of crystallographic shear planes which accommodate changes in the oxygen/metal ratio by switching from corner sharing to edge sharing (and conversely) of some of the oxygen ion octahedra in the structure (*2, 5, 9–13*). According to this scheme structural rearrangements accompanying reduction consist in the elimination of oxygen vacancies formed at the initial stage and in consequence change substantially the local environment of the molybdenum ions involved.

The ESR spectroscopy has been extensively used for investigation of the molybdenum valences distribution and also for determination of the local environment of the paramagnetic molybdenum species (*14–24*). The analysis of g-tensor which is derived from the resonance fields yields direct information about the symmetry of crystal field surrounding the paramagnetic centre.

In the present paper the results of carefully performed ESR investigation of MoO_3 reduction are reported, which provide considerable support for the suggested "crystallographic shear" mechanism of MoO_3 reduction.

Experimental

The polycrystalline MoO_3 (Merck, pro analysi) placed in quartz EPR tubes was

0022-4596/84 $3.00

Copyright © 1984 by Academic Press, Inc.
All rights of reproduction in any form reserved.

heated in air at 703 K for 1 hour, subsequently connected to the vacuum line equipped with greaseless stopcocks, outgassed at room temperature for 1 hour and submitted to heat treatment at 703 K under vacuum of 10^{-3} Pa for different periods of time ranging from 5 to 60 minutes. The samples were then studied in the ESR spectrometer. Subsequently the reduced samples were submitted to reoxidation in air and the ESR spectra were recorded after each oxidizing treatment.

ESR analysis. The spectra were recorded at 77 K, as well as in the temperature range 123 K – 293 K by using a Varian E-line Century Series spectrometer model E-112 operating in the X-band and a variable temperature accessory V-4557 (available in the Institute of Physical Chemistry of Kiel University, Federal Republic of Germany) and on an ESR X-band spectrometer type SE/X (available in the Institute of Chemistry of Jagiellonian University, Krakow, Poland). Spin densities were estimated by use of a $VOSO_4$ standard. DPPH sample (g = 2.0036) was used for determination of the g values.

Results

The samples of polycrystalline MoO_3, after an initial oxidizing treatment, were white and did not show any ESR signal, indicating a stoichiometric composition for the compound. Heating *in vacuo* at 703 K resulted in change of color to white-grayish or gray for strongly reduced preparations. All MoO_3 samples reduced in this way exhibited ESR signals, which differed considerably depending on the degree of reduction, i.e., time of applied heat treatment.

Figure 1 (solid line) shows the ESR spectrum recorded at 77 K of MoO_3 treated *in vacuo* at 703 K for 5 min. The shape of the signal represents an asymmetrical line indicating local crystal field of nonaxial symmetry. Analysis of the spectrum leads to the following magnetic parameters: $g_x = 1.946$, $g_y = 1.960$ (corresponding to $g_\perp$), and $g_z = 1.868$ (corresponding to $g_\parallel$). Only very weak poorly resolved satellite absorptions, possibly due to the hyperfine structure resulting from the 25% abundant ^{95}Mo and ^{97}Mo isotopes with nuclear spin $I = \frac{5}{2}$, are observed. This signal is denoted as signal A.

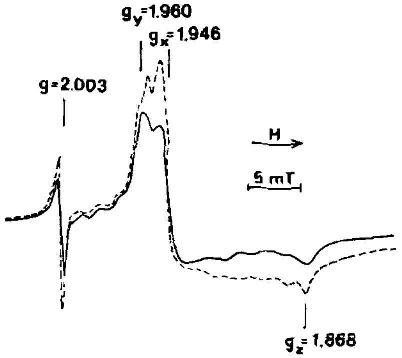

FIG. 1. ESR spectra of MoO_3 reduced *in vacuo* at 703 K: — 5-min treatment; ---, 8-min treatment.

The ESR spectrum of the sample treated *in vacuo* for 8 min shows some additional features, indicating the superposition of another spectrum with different g tensor asymmetry (Fig. 1, dashed line). This new spectrum, denoted B, becomes more intense with time of reduction. For the sample heated for 35 min, the spectrum presented in Fig. 2 (solid line) is obtained. This signal is characterized by $g_x = 1.943$, $g_y = 1.954$, and $g_z = 1.878$. Well-resolved hyperfine structure corresponding to the natural abundance of odd Mo isotopes allowed determination of the hyperfine splitting constants $A_x = 3.2$ mT, $A_y = 3.0$ mT, and $A_z = 7.0$ mT. The calculated magnetic parameters of the A and B spectra enabled assignment of them to Mo(V) species in a nonaxial environment differing slightly by a degree of crystal field distortion.

Further heating *in vacuo* led to an increase of signal B integral intensity accompanied by ESR line broadening. This re-

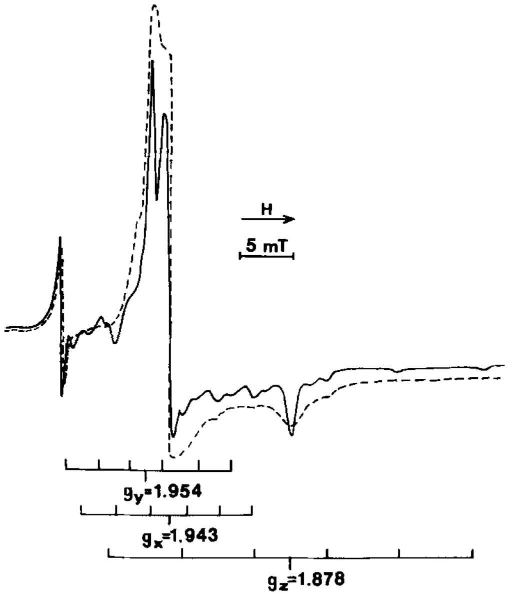

FIG. 2. ESR spectra of MoO_3 reduced *in vacuo* at 703 K: — 35-min treatment; ---, 60-min treatment.

sulted in disappearance of the hyperfine pattern and worse resolution of perpendicular g tensor components (Fig. 2, dashed line).

In all vacuum-treated samples a narrow single line with $g = 2.003$ was observed. Similar signals have been noted previously for various oxides (*19, 25–29*). There is no unequivocal interpretation of this absorption. *F* centers, carbon impurities, O^- ions, or organic radicals can be responsible for this. In the present case the oxidizing pretreatment of MoO_3 samples as well as the use of a greaseless vacuum system seems to eliminate the possibility of carbon impurities. On the other hand, the saturation properties of the signal and its diminishing upon contact with air led us to ascribe absorption around $g = 2.003$ to the singly ionized oxygen vacancy. The exact nature of this signal is being studied presently and the results will be published in a separate paper.

Reoxidizing treatment tended to reverse the changes in the ESR spectra. Readmission of air at room temperature slightly improved the resolution of signal B (Fig. 3a). A subsequent 5-min heating at 703 K resulted in decrease of the ESR signal intensity. Simultaneously, features characteristic of signal A appeared on the background of signal B absorption (Fig. 3b). Further oxidation at 703 K for 15 min led to the appearance of a pure A signal, its intensity decreasing with time of reoxidation (Fig. 3c), up to complete vanishing after 90 min treatment.

Adsorption of water vapor at room temperature by a MoO_3 sample pretreated for 5 min *in vacuo* at 703 K led to the partial conversion of signal A present in this preparation to signal B. Contact with water vapor had no substantial influence on the ESR spectra of stronger reduced samples.

Discussion

In the reduced MoO_3 system several valence states of molybdenum ions are possible. Mo(VI) is diamagnetic and therefore inactive in ESR. Mo(IV) is a non-Kramers

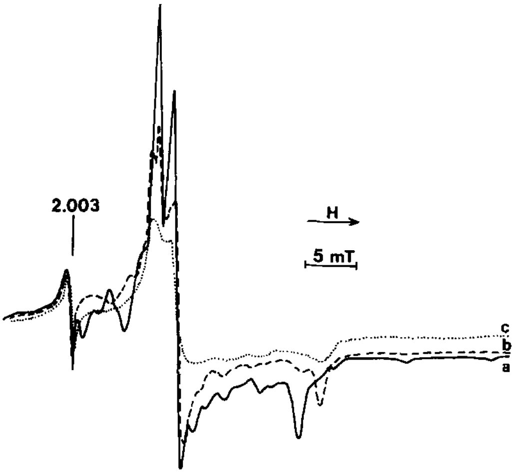

FIG. 3. ESR spectra of MoO_3 reduced for 35 min at 703 K and subsequently submitted to reoxidation: (a) —, after contact with air at room temperature; (b) ---, after 5 min in air at 703 K; (c) ···, after 15 min in air at 703 K.

ion and in its possible environment in MoO_3 is not expected to give the ESR signal. ESR spectra of Mo(III) in the oxide matrix have already been reported and their parameters differ substantially from the present results (*30*). On the other hand the presence of Mo(V) generally observed in the reduced molybdena containing systems was manifested in the ESR spectra as an asymmetrical signal with $g_{\parallel} = 1.85–1.92$ and $g_{\perp} = 1.92–1.95$ (*14–24*). Therefore the signals A and B reported here have been assigned to Mo(V) ions in two different environments of nonaxial symmetry.

In order to interpret the obtained ESR data it is necessary to discuss briefly the crystallographic structure of MoO_3. The molybdena lattice is a layer structure built up of distorted MoO_6 octahedra. The distortion of the MoO_6 unit is caused by the off-center displacement of the metal atom toward one of the surrounding oxygens (*31*). Localization of an additional electron on a molybdenum(VI) site, i.e., formation of Mo(V), leads to a situation which, considering the coordination of molybdenum, is similar to that encountered in molybdenyl complexes (*32–34*). The energy level diagram of the molecular orbitals for such complexes has been calculated by Ballhausen and Gray assuming C_{4v} symmetry (*32*). Because of rhombic distortion of MoO_6 elementary octahedra, the C_{2v} symmetry provides a better structural description (*21*). Figure 4 shows the energy level diagram of the Mo(V) d^1 ion in the ligand field of C_{2v} symmetry. The paramagnetic electron is located in the $a_2(xy)$ orbital with mainly molybdenum d_{xy} character. In the case of species B a reasonable value of 0.85 for spin density in d_{xy} was found by comparison of the experimentally determined hyperfine anisotropic parameter $P_{\mathrm{exp}} = \frac{7}{6}(A_{\perp} - A_{\parallel})$ equal to 127.4 MHz with the theoretically computed value of $P_{\mathrm{theor.}} = 150.7$ MHz given by Morton and Preston (*35*).

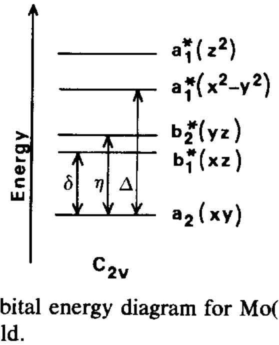

FIG. 4. Orbital energy diagram for Mo(V) d^1 ion in C_{2v} ligand field.

The *g* values and the ligand field energies are interrelated by the approximate equations

$$g_z = g_e - \frac{8\lambda}{\Delta}, \tag{1}$$

$$g_x = g_e - \frac{2\lambda}{\delta}, \tag{2}$$

$$g_y = g_e - \frac{2\lambda}{\eta}, \tag{3}$$

where g_e is the free electron g value, λ is the spin-orbit coupling constant of molybdenum ion, and Δ, δ, and η are the energies attributed to the optical transitions $a_2(xy) \rightarrow a_1^*(x^2 - y^2)$, $a_2(xy) \rightarrow b_1^*(xz)$, and $a_2(xy) \rightarrow b_2^*(yz)$, respectively. Parameter Δ corresponds to the 10-Dq splitting in the octahedral crystal field, δ reflects the degree of tetragonal distortion, whereas η determines the magnitude of rhombic distortion. The spin-orbit coupling constant for the Mo(V) in MoO_3 has been determined to be 375 cm^{-1} and is about 35% of the free ion value (*14*). Such a strong reduction is common for oxycations and is due to the covalency effects (*32–34*).

Substituting the *g* factor components determined for species A and B from their ESR spectra in Eqs. (1), (2), and (3) the crystal field parameters of the nearest surrounding of respective Mo(V) centers may be evaluated. Suitable calculations give for centers A $\Delta_A = 22{,}500$ cm^{-1}, $\delta_A = 13{,}500$ cm^{-1}, $\eta_A = 17{,}500$ cm^{-1}, and for centers B

$\Delta_B = 24{,}000\ \text{cm}^{-1}$, $\delta_B = 12{,}500\ \text{cm}^{-1}$, $\eta_B = 15{,}500\ \text{cm}^{-1}$. From optical measurements it is known that for the pentacoordinated Mo(V) oxycation in an oxide matrix, Δ is equal to 21,800–22,100 cm^{-1}, δ = 13,800 cm^{-1}, and η = 16,700 cm^{-1} (*21*). Comparison of crystal field parameters calculated from the g formulas with experimental data shows that computed values are close to the experimental results, the agreement being strikingly good for A-type Mo(V) species. This would indicate that the $(MoO_5)^{5-}$ cluster (i.e., Mo(V) ion in rhombically distorted tetragonal pyramid adjacent to an oxygen vacancy opposite to molybdenyl oxygen) is responsible for the ESR signal denoted previously as signal A. On the other hand the crystal field parameters calculated for the surrounding of B species reveal considerably lower tetragonal and rhombic distortion ($\delta_A > \delta_B$, $\eta_A > \eta_B$), indicating the increase of the local symmetry with respect to A centers. An ESR signal identical to that of spectrum B was observed by us for the same MoO_3 preparations reduced with atomic hydrogen at room temperature (*36*). There the experimental conditions provided samples with fully occupied anionic sites resulting in octahedral environment of Mo(V). Spectrum B may be ascribed to the $(MoO_6)^{7-}$ cluster of octahedrally coordinated Mo(V) ion.

Adsorption of water vapor and some other polar compounds is known to influence the ESR spectra of coordinatively unsaturated transition metal ions due to the completion of their coordination sphere (*37, 38*). The appearance of signal B in the ESR spectrum of slightly reduced MoO_3 after contact with H_2O and the diminishing of signal A reflect the improvement of the local symmetry of Mo(V) ions involved. This is consistent with the assumption that the adsorbed water molecule enters the nearest surrounding of the pentacoordinated $(MoO_5)^{5-}$ site and adjusts the symmetry of the latter to the distorted octahedron. It also indicates that the pentacoordinated Mo(V) centers are localized mainly at the surface of MoO_3 crystallites. Thus the result of the adsorption experiment confirms our previous considerations.

Identification of centers A and B as pentavalent molybdenum in distorted pyramidal and octahedral coordinations, respectively, implies the possible interpretation of reported ESR experiments in terms of crystallographic shear effect occurring in MoO_3 upon reduction.

ESR spectra demonstrate clearly that at the initial stage of reduction pentacoordinated Mo(V) ions adjacent to an oxygen vacancy are formed at the surface of MoO_3 crystallites (Fig. 1). The appearance of Mo(V) in octahedral surrounding after further reduction (Fig. 2) is explained in terms of elimination of oxygen vacancies due to the switch of structural polyhedra from corner to edge sharing. This rearrangement is responsible for the change in molybdenum coordination number from 5 to 6. Prolonged reduction resulted in worse resolution of the ESR spectra due to the high concentration of paramagnetic species and increasing dipolar broadening effects. Subsequent reoxidation led to the reverse structural changes. Contact with air at room temperature improved the resolution of the ESR spectrum most probably due to the partial depletion of paramagnetic species responsible for the ESR absorption. Brief heating in air at 703 K led to an intermediate situation—the intensity of octahedrally coordinated species decreased and simultaneously the signal characteristic for the Mo(V) in distorted square pyramidal surrounding appeared again in the ESR spectrum (Fig. 3b). Such behavior indicates that shear structures become destroyed upon oxidizing treatment at 703 K. In the course of structure reconstruction paramagnetic defects such as pentacoordinated molybdenyl ions are created, being responsible for oxygen deficiency in the final stage of reoxidation (Fig. 3c). The total disappearance of the ESR signal after 90 min of oxidizing treatment corresponds to the restoration of the stoichiometric composition of the MoO_3 sample.

Conclusions

The occurrence of Mo(V) molybdenyl ions either in rhombically distorted square pyramid coordination with one vacant oxygen position or in rhombically distorted octahedral surrounding of oxygen ions has been found in reduced MoO_3 by means of ESR spectroscopy. The former centers appeared at the very early stages of reduction, whereas the latter, indicating structural rearrangements, were observable in the more strongly reduced samples. Reoxidation resulted in the reverse changes. Present ESR results give strong support to the suggested shear mechanism for MoO_3 reduction.

Acknowledgments

I wish to thank Professor J. Haber, Institute of Catalysis and Surface Chemistry, Polish Academy of Sciences, Krakow, Poland, for stimulating discussions and critical reading of the manuscript. Thanks are also due to Professor R. N. Schindler, Institute of Physical Chemistry, Kiel University, Federal Republic of Germany, for his kind agreement to use the ESR equipment in his laboratory.

References

1. P. A. Batist, C. J. Kapteijns, B. C. Lippens, and G. C. A. Schuit, *J. Catal.* **7,** 33, (1967).
2. L. A. Bursill, *Proc. R. Soc. London* **311,** 267 (1969).
3. F. E. Massoth, *J. Catal.* **30,** 204 (1973).
4. T. Fransen, P. C. van Berge, and P. Mars, *React. Kinet. Catal. Lett.* **5,** 445 (1976).
5. W. Thöni, P. Gai, and P. B. Hirsch, *J. Less-Common Met.* **54,** 263 (1977).
6. R. Burch, *J. Chem. Soc. Trans. 1* **74,** 2982 (1978).
7. E. L. Aptekar, M. G. Chudinov, A. M. Alekseev, and O. V. Krylov, *React. Kinet. Catal. Lett.* **1,** 493 (1974).
8. N. Giordano, A. Castellan, J. C. J. Bart, A. Vaghi, and F. Campadelli, *J. Catal.* **37,** 204 (1975).
9. J. Haber, W. Marczewski, J. Stoch, and L. Ungier, *Ber. Bunsenges. Phys. Chem.* **79,** 970 (1975).
10. A. Cimino and B. A. de Angelis, *J. Catal.* **36,** 11 (1975).
11. F. S. Stone, *J. Solid State Chem.* **12,** 271 (1975).
12. E. Brocławik, A. E. Foti, and V. H. Smith, *J.* Catal. **51,** 380 (1978). E. Brocławik, A. E. Foti, and V. H. Smith, *J. Catal.* **67,** 103 (1981).
13. J. Haber, *J. Less-Common Met.* **54,** 243 (1977).
14. V. A. Joffe, I. B. Patrina, E. V. Zelenetskaya, and V. P. Mikheyeva, *Phys. Status Solidi* **35,** 535 (1969).
15. G. N. Asmolov and O. V. Krylov, *Kinet. Katal.* **13,** 188 (1972).
16. K. S. Seshadri and L. Petrakis, *J. Catal.* **30,** 195 (1973).
17. R. S. Mann and K. C. Khulbe, *Bull. Chem. Soc. Japan* **48,** 1021 (1975).
18. S. Abdo, M. Lo Jacono, R. B. Clarkson, and W. K. Hall, *J. Catal.* **36,** 330 (1975).
19. L. Burlamacchi, G. Martini, F. Trifiro, and G. Caputo, *J. Chem. Soc. Faraday Trans. 1* **71,** 209 (1975).
20. M. Che, F. Figueras, M. Forissier, J. McAteer, M. Perrin, J. L. Portefaix, and H. Praliaud, *in* "Proceedings, 6th International Congress on Catalysis, London, 1976," paper A17.
21. J. Hanuza, B. Jeżowska-Trzebiatowska, and W. Oganowski, *Bull. Acad. Pol. Sci. Ser. Sci. Chim.* **25,** 569 (1977); J. Hanuza, B. Jeżowska-Trzebiatowska, and W. Oganowski, *Bull. Acad. Pol. Sci. Ser. Sci. Chim.* **25,** 735 (1977).
22. M. Che, J. C. McAteer, and J. Tench, *J. Chem. Soc. Faraday Trans. 1* **74,** 2378 (1978).
23. L. Petrakis, P. L. Meyer, and T. P. Debies, *J. Phys. Chem.* **84,** 1020 (1980).
24. M. Che, B. Canosa, and A. R. Gonzalez-Elipe, *J. Chem. Soc. Faraday Trans. 1* **78,** 1043 (1982).
25. J. H. C. van Hoof, *J. Catal.* **11,** 277 (1968).
26. K. Tarama, S. Yoshida, S. Ishida, and Y. Doi, *Bull. Chem. Soc. Japan* **42,** 1161 (1969).
27. C. Naccache, P. Meriaudeau, M. Che, and A. J. Tench, *Trans. Faraday Soc.* **67,** 506 (1971).
28. K. M. Sancier, T. Dozono, and H. Wise, *J. Catal.* **23,** 270 (1971).
29. E. Serwicka, M. W. Schlierkamp, and R. N. Schindler, *Z. Naturforsch. A* **36,** 226 (1981).
30. W. D. Ohlsen, *Phys. Rev. B* **7,** 4058 (1973).
31. L. Khilborg, *Ark. Kem.* **21,** 357 (1963).
32. C. J. Ballhausen and H. B. Gray, *Inorg. Chem.* **1,** 111 (1962); H. B. Gray and C. R. Hare, *Inorg. Chem.* **1,** 363 (1962).

33. K. De Armond, B. B. Garrett, and H. S. Gutowsky, *J. Chem. Phys.* **42,** 1019 (1965).
34. P. T. Manoharan and M. T. Rogers, *J. Chem. Phys.* **49,** 5510 (1968).
35. J. R. Morton and K. F. Preston, *J. Magn. Reson.* **30,** 577 (1978).
36. E. Serwicka and R. N. Schindler, *Z. Phys. Chem. N.F.* **133,** 175, (1982).
37. V. M. Vorotyntsev, V. A. Shvets, and V. B. Kazanskii, *Kinet. Katal.* **12,** 1249 (1971).
38. M. Che, M. Fournier, and J. P. Launay, *J. Chem. Phys.* **71,** 1954 (1979).